Journal of Marine Science and Technology

Volume 21 | Issue 1 Article 10

FLEXURAL STRENGTH OF PRESTRESSED CONCRETE BEAMS WITH TENDON WRAPPED BY PLASTIC SHEETS

Ta-Heng Wang
Department of Harbor and River Engineering, National Taiwan Ocean University, Keelung, Taiwan, R.O.C, big-sky@umail.hinet.net

Ran Huang
Department of Harbor and River Engineering, National Taiwan Ocean University, Keelung, Taiwan, R.O.C

Jiang-Jhy Chang
Department of Harbor and River Engineering, National Taiwan Ocean University, Keelung, Taiwan, R.O.C

Journal of Marine Science and Technology, Vol. 21, No. 1, pp. 76-81 (2013)
DOI: 10.6119/JMST-011-1226-1

FLEXURAL STRENGTH OF PRESTRESSED CONCRETE BEAMS WITH TENDON WRAPPED BY PLASTIC SHEETS

Ta-Heng Wang, Ran Huang, and Jiang-Jhy Chang

Key words: unbonded tendon, prestressed concrete beam, flexural strength, crack width.

ABSTRACT

For post-tension prestressed concrete beams, both of tendons laid in metal duct and wrapped by plastic sheets are recognized as unbonded tendon by researchers, and the same equation is used to estimate the flexural strength. But the contacting conditions between tendon and its surrounding concrete are quite different for these two kinds of unbonded tendons. This study compares the flexural strength, crack distribution and crack width of beams with these two kinds of unbonded tendons and bonded tendon. The results reveal that the structural behavior of tendon wrapped by plastic sheets is between bonded tendon and tendon laid in metal duct. A modified equation is proposed to estimate flexural strength of tendon wrapped by plastic sheets. Reducing cost and shortening construction time are the main advantages for this kind of the prestressed beams with tendon wrapped by plastic sheets. After further investigation, it may be an alternative method for the post-tension prestressed concrete structure in the future.

I. INTRODUCTION

Generally, both of tendon erected in metal duct without grouting (TWOG) and tendon wrapped by plastic sheets (TWP) are normally recognized as unbonded tendons by researchers [5, 8]. However, it is obvious that the contacting conditions between tendon and its surrounding concrete are quite different between TWOG and TWP. For TWP, in addition to separate from some thin layers of plastic sheets, tendon and concrete nearly contact with each other. And due to concrete pouring, some contacting pressure and friction may exist between them. But for TWOG, tendon is laid in a metal duct with a relatively lager diameter than tendon, and does not contact with surrounding concrete at all. In the design of prestressed concrete beams, the nominal flexural strength φ Mn is computed by using strength equations similar to those for non-prestressed concrete beams. Since 1977, American Concrete Institute (ACI) proposed an equation for calculating the flexural stress of unbonded tendon for beam with a span-to-depth ratio ≦35. This equation is used for both of TWOG and TWP.

For a prestressed concrete beam with bonded tendon at loading, the change in strain at the point of consider in the tendon is equal to the local adjacent concrete. Hence the stress at different point along the tendon may not be the same. Strain compatibility method can be used to estimate the flexural stress of the tendon. But in case of unbonded tendon, the change in strain in the tendon is equal to the average strain of the adjacent concrete over the whole beam. So the stress at every point along the tendon is equal and strain compatibility method is invalid. This was first proposed by Baker [3] in 1949. For estimating f_{ps} of unbonded prestressed concrete beam, Warwaruk [9] has plotted the relationship between (f_{ps}-f_{se}) *vs.* ρ_p / f_c' and developed an approximate equation as illustrated as Eq. (1a) or (1b). Where f_{se} is the effective stress in prestressing steel, ρ_p is the ratio of A_{ps} to bd_p, b is the width of compression member, d_p is the distance from extreme compression fiber to centroid of prestressing steel, and f_c' is the specified compressive strength of concrete.

$$f_{ps} = f_{se} + (30{,}000 - 10^{10} \rho_p / f_c') \quad psi \tag{1a}$$

$$f_{ps} = f_{se} + (215 - 49.5 \times 10^5 \rho_p / f_c') \quad MPa \tag{1b}$$

In 1963, ACI Code suggested an approximate equation shown as Eq. (2a) or (2b)

$$f_{ps} = f_{se} + 15{,}000 \quad psi \tag{2a}$$

$$f_{ps} = f_{se} + 108 \quad MPa \tag{2b}$$

Paper submitted 03/16/11; revised 12/12/11; accepted 12/26/11. Author for correspondence: Ta-Heng Wang (e-mail: big-sky@umail.hinet.net).
Department of Harbor and River Engineering, National Taiwan Ocean University, Keelung, Taiwan, R.O.C.

In 1971, based on the testing results of 9 testing beams with prestressed unbonded tendons erected in a 3/4” circular tube without grouting, Mattock *et al*. [6] indicated that the computed results from both Eq. (1) and Eq. (2) were too conservative and suggested an approximate equation as follow:

$$f_{ps} = f_{se} + 70 + 1.4\frac{f'_c}{\rho_p} \quad MPa \tag{3}$$

Eq. (3) was simplified and proposed by the ACI-ASCE Joint Committee 423 [4] as Eq. (4).

$$f_{ps} = f_{se} + 70 + \frac{f'_c}{\rho_p} \quad MPa \tag{4}$$

Mojahidin and Gamble [7] introduced an additional span to depth ratio factor to Eq. (4) in 1978. Based on Mojahidin’s conclusion, until now ACI (ACI318-08 [1]) still use Eq. (5) for members with a span-to-depth ratio of ≦35 and Eq. (6) for members with a span-to-depth ratio greater than 35, to predict f_{ps} respectively. And for bonded tendons, ACI proposed an approximate Eq. (7) to predict f_{ps} if f_{se} is not less than 0.5 f_{pu}.

$$f_{ps} = f_{se} + 70 + \frac{f'_c}{100\rho_p} \le f_{py}$$
$$nor \le (f_{se} + 420) \quad MPa \tag{5}$$

$$f_{ps} = f_{se} + 70 + \frac{f'_c}{300\rho_p} \le f_{py}$$
$$nor \le (f_{se} + 210) \quad MPa \tag{6}$$

$$f_{ps} = f_{pu}\left\{1 - \frac{\gamma_p}{\beta_1}\left[\rho_p \frac{f_{pu}}{f'_c} + \frac{d}{dp}(\omega - \omega')\right]\right\} \quad MPa \tag{7}$$

where f_{pu} is specified tensile strength of prestressing steel, γ_p is factor for type of prestressing steel, β_1 is factor relating depth of equivalent rectangular compressive stress block to neutral axis depth, ω is tension reinforcement index and ω' is compression reinforcement index.

In 2004, Au and Du [2] proposed Eq. (8a) and Eq. (8b) to predict f_{ps} of TWOG. Where E_{ps} is modulus of elasticity of prestressing steel and l_e is the length of the tendon between the end anchorages divided by the number of plastic hinges n required to develop a failure mechanism in the span under consideration.

$$f_{ps} = f_{se} + \frac{0.0279\, E_{ps}(dp - cpe)}{l_e} \le f_{py} \quad MPa \tag{8a}$$

where

$$cpe = \frac{A_{ps} f_{se} + A_s f_y}{0.85\, \beta_1 f'_c b} \tag{8b}$$

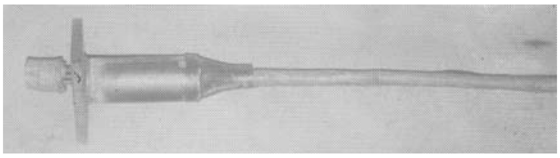

Fig. 1. Tendon wrapped by plastic sheet.

Based on the different contacting condition between TWOG and TWP, this study assumes that the ACI equation mentioned above may be too conservative for TWP. In this study, 20 prestressed concrete beams (18 beams with TWP, 1 beam with TWOG, and 1 beam with bonded tendon) were tested to investigate the different behavior of TWOG and TWP. In addition to propose an equation to estimate the steel stress f_{ps} at nominal flexural strength, the comparisons of crack distribution and crack width between TWP and TWOG are also discussed below.

II. EXPERIMENTAL PROGRAM

1. Materials

φ 7 mm uncoated stress-relieved wires which meet the requirements of ASTM A421 are used as prestressing steel. And non-prestressed steel is conform to ASTM A615M. For minimizing the loss due to prestressing steel seating at transfer, BBRV Wire Post-tensioning System is chosen. The TWP tendonss are composed by several wires which are coated grease and wrapped by plastic sheets. One set of anchorage and tendon is shown in Fig. 1.

2. Specimens

There are 20 specimens (12 rectangular beams and 8 T-beams) with the same 360 cm effective length and 30 cm height are used in this test. The tendons of beams are embedded as parabolic which is zero eccentricity at both ends and with an eccentricity 8.9 cm for rectangular beams, 11.4 cm for T-beams at mid-span. The geometries of specimens are shown in Fig. 2 and details are listed in Table 1. The designations of specimens listed in Table 1 indicate: R/T: Rectangular/Tee beam; 1st Arabic number: number of φ 7 mm wires; 2nd Arabic number: number of non-prestressing steel; 3rd Arabic number: designation of non-prestressing steel; P: TWP; U: TWOG; B: bonded.

Five dial gauges are erected under the beams to measure the deflections during loading. Additionally several strain gauges are adhered to the top face of concrete beams, prestressing steel, tension and compression non-prestressed reinforcement steel. The positions of dial gauges (micrometer) and strain gauges are shown in Fig. 3.

3. Experimental Procedures

The specimens are loaded by two equal loadings at 1/3 effective length as shown in Fig. 3. The loading are applied to the specimens to failure with increment of 10 KN. Fig. 4 shows testing conditions of specimens R5 and T3.

Table 1. Deatails of specimens.

Specimen No.	Designation	A_{ps} (cm^2)	A_s (cm^2)	A_s' (cm^2)	f_c' (MPa)	dp (cm)	d (cm)	Jack forces (KN)
R1	R300-P	1.161	0.000	1.42	26.50	23.89	26.00	126.55
R4	R323-P	1.161	1.420	1.42	24.46	23.89	26.00	132.63
R2	R500-P	1.940	0.000	1.42	26.50	23.89	26.00	176.91
R5	R523-P	1.940	1.420	1.42	24.46	23.89	26.00	196.89
R9	R523-P	1.940	1.420	1.42	29.56	23.89	26.00	210.99
R10	R523-P	1.940	1.420	1.42	24.46	23.89	26.00	207.47
R8	R525-P	1.940	3.960	1.42	29.56	23.89	25.50	203.95
R7	R524-P	1.940	2.540	1.42	29.56	23.89	25.80	210.98
R3	R700-P	2.709	0.000	1.42	26.50	23.89	26.00	217.96
R6	R723-P	2.709	1.420	1.42	24.46	23.89	26.00	235.66
T1	T300-P	1.161	0.000	1.42	26.50	23.58	26.00	122.79
T4	T323-P	1.161	1.420	1.42	24.46	23.58	26.00	119.49
T2	T500-P	1.940	0.000	1.42	26.50	23.58	26.00	196.92
T5	T523-P	1.940	1.420	1.42	29.56	23.58	26.00	211.02
T7	T524-P	1.940	2.540	1.42	24.46	23.58	25.80	196.92
T8	T525-P	1.940	3.960	1.42	24.46	23.58	25.50	240.39
T3	T700-P	2.709	0.000	1.42	24.46	23.58	26.00	227.18
T6	T723-P	2.709	1.420	1.42	29.56	23.58	26.00	284.90
R11	R523-U	1.940	1.420	1.42	24.46	23.89	26.00	210.99
R12	R523-B	1.940	1.420	1.42	24.46	23.89	26.00	221.55

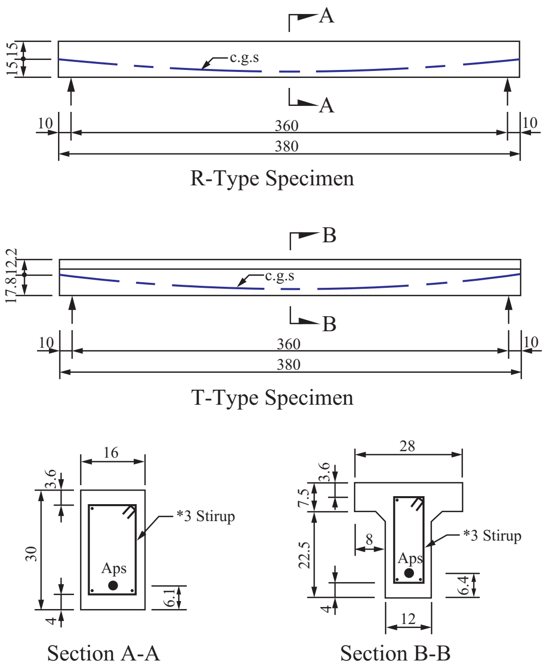

Fig. 2. Elevations and Sectional profiles of specimens.

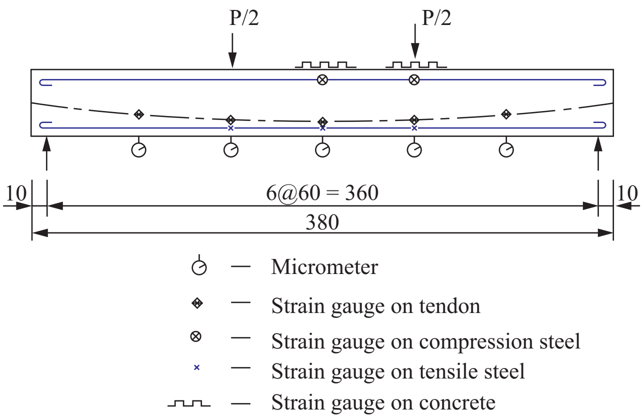

Fig. 3. Layout of strain gauges and micrometers.

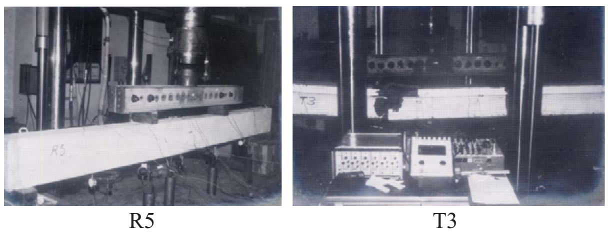

Fig. 4. Set-up of Beams under testing.

During testing, all strains of tendon, non-prestressing steel and concrete are recorded by computer data acquisition system at each loading stage automatically. Meanwhile the computer captures the beam deflection data from 5 micrometers which are also automatically recorded until failure. But, the location and width of each crack on concrete face at each loading are measured by inspection.

III. RESULTS AND DISCUSSION

1. Flexural Strength

Only 7 strain gauges adhered to the tendons of 7 specimens

Table 2. Comparison of f_{ps}.

Specimen No.		Measured		Strain compatibility		Eq. (7)		Eq. (5)		Eq. (8)		Proposed Eq. (9)	
		ε_{ps} ($\times 10^{-6}$)	f_{ps}	f_{ps}	ratio	f_{ps}	ratio	f_{ps}	ratio	f_{ps}	ratio	f_{ps}	ratio
R1	R300-P	-	-	1,658	-	1,497	-	1,177	-	1,323	-	1,346	-
R4	R323-P	0.00775	1,465	1,624	0.902	1,463	1.001	1,219	1.202	1,341	1.092	1,346	1.088
R2	R500-P	0.00575	1,147	1,580	0.726	1,387	0.827	975	1.177	1,130	1.015	1,222	0.939
R5	R523-P	-	-	1,559	-	1,316	-	1,067	-	1,185	-	1,315	-
R9	R523-P	0.00683	1,344	1,589	0.846	1,379	0.975	1,145	1.174	1,270	1.059	1,346	0.999
R10	R523-P	0.00770	1,460	1,565	0.933	1,316	1.110	1,118	1.305	1,230	1.187	1,346	1.085
R8	R525-P	-	-	1,558	-	1,310	-	1,111	-	1,206	-	1,346	-
R7	R524-P	-	-	1,578	-	1,349	-	1,145	-	1,255	-	1,346	-
R3	R700-P	-	-	1,467	-	1,253	-	860	-	1,008	-	1,061	-
R6	R723-P	0.00569	1,136	1,410	0.806	1,171	0.970	918	1.237	1,027	1.105	1,119	1.015
T1	T300-P	-	-	1,731	-	1,409	-	1,124	-	1,318	-	1,346	-
T4	T323-P	-	-	1,687	-	1,359	-	1,092	-	1,276	-	1,346	-
T2	T500-P	0.00687	1,351	1,649	0.819	1,225	1.102	1,058	1.277	1,256	1.076	1,284	1.052
T5	T523-P	-	-	1,651	-	1,250	-	1,130	-	1,315	-	1,346	-
T7	T524-P	0.00732	-	1,611	-	1,139	-	1,055	-	1,228	-	1,274	-
T8	T525-P	0.00917	1,540	1,628	0.946	1,113	1.385	1,265	1.218	1,346	1.145	1,346	1.144
T3	T700-P	-	-	1,583	-	991	-	880	-	1,076	-	1,057	-
T6	T723-P	-	-	1,608	-	1,088	-	1,084	-	1,262	-	1,296	-
	Average for TWP				0.854		1.053		1.227		1.097		1.046
R11	R523-U	-	-	-	-	-	-	1,135	-	1,245	-	1,346	-
R12	R523-B	-	-	1,574	-	1,316	-	-	-	-	-	-	-

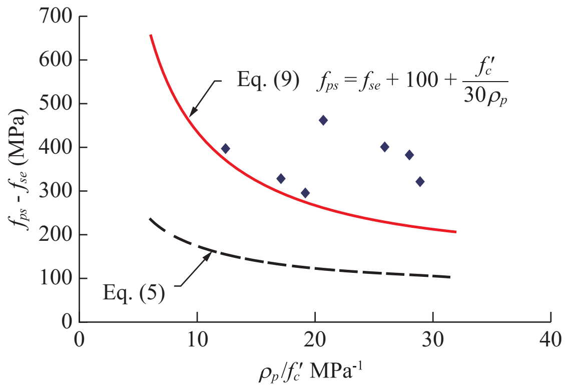

Fig. 5. (f_{ps}-f_{se}) vs. ρ_p/f_c' curves for TWP beams.

are recorded successively during the testing. These 7 captured strains (ε_{ps}) and their respective stresses (f_{ps}) which are calculated from strain-stress relationship are listed in the second and third columns of Table 2. The other f_{ps} calculated by equations mentioned above are also listed in Table 2 for comparison. It shows f_{ps} calculated by Eq. (5) proposed by ACI is 1.227 times to measured values.

Since the total losses of prestressed tendon is hard to be measured during testing, in this study f_{se} is assumed to be equal to 90% of initial prestressing stress f_{si}. As Warwaruk's research [9], values calculated by Eq. (5) and values calculated by Eq. (9) proposed by this study are shown in Fig. 5 for comparison. It is obvious that f_{ps} calculated by Eq. (5) is too conservative, and Eq. (9) is a lower bound equation. Meanwhile as shown in Table 2 using Eq. (9) to predict f_{ps} with an average value of 1.046 will be more closer to the measured values than using the other equations.

$$f_{ps} = f_{se} + 100 + \frac{f_c'}{30\,\rho_p} \le f_{py}$$

$$nor \le (f_{se} + 420) \quad MPa \tag{9}$$

Meanwhile another comparisons of testing failure moments to nominal moment Mn calculated by f_{ps} listed in Table 2 is also shown in Table 3. It reveals three conclusions:

(1) Although the 5 specimens of R5, R9, R10, R11 and R12 are designed with the same amount of tendon and non-prestressing steel, but those have different moment capacities. R12 beam with bonded tendon possesses the greatest failure moment 71.34 KN-m, R11 beam with TWOG failures at the smallest moment 62.45 KN-m, and the failure moments of R5, R9, R10 beams with TWP are between R12 and R11. This result proves the assumption mentioned above that the behavior of beam with TWP would be between beam with bonded tendon and with TWOG.

(2) In Table 3, it also shows that the nominal moment Mn calculated by strain compatibility for beams with TWP is very close to testing failure moment with an average ratio 1.014. It also reveals that nominal moments for beams with TWP predicted by Eq. (5) suggested by ACI for

Table 3. Comparison of Mn.

Specimen No.		Test	Strain compatibility		Eq. (7)		Eq. (5)		Eq. (8)		Proposed Eq. (9)	
		Mn (KN-m)	Mn (KN-m)	Ratio	Mn (KN-m)	Ratio	Mn (KN-m)	Ratio	Mn (KN-m)	Ratio	Mn (KN-m)	Ratio
R1	R300-P	44.15	41.24	1.07	37.65	1.173	30.11	1.466	33.388	1.322	34.12	1.294
R4	R323-P	52.97	48.74	1.09	45.37	1.168	39.90	1.328	42.195	1.255	42.77	1.239
R2	R500-P	61.80	62.27	0.99	55.78	1.108	40.69	1.519	46.484	1.330	49.89	1.239
R5	R523-P	67.69	68.41	0.99	60.71	1.115	52.30	1.294	55.511	1.219	60.69	1.115
R9	R523-P	65.16	71.30	0.91	64.35	1.013	56.11	1.161	59.990	1.086	63.22	1.031
R10	R523-P	64.33	68.57	0.94	60.71	1.060	54.08	1.190	56.861	1.131	61.68	1.043
R8	R525-P	82.64	82.96	1.00	75.34	1.097	68.91	1.199	70.789	1.167	76.46	1.081
R7	R524-P	79.11	76.75	1.03	69.41	1.140	62.51	1.266	65.391	1.210	69.32	1.141
R3	R700-P	78.28	77.10	1.02	67.78	1.155	49.12	1.594	56.531	1.385	59.03	1.326
R6	R723-P	81.82	80.38	1.02	70.50	1.160	59.60	1.373	63.538	1.288	68.39	1.196
T1	T300-P	47.09	44.17	1.07	36.31	1.297	29.17	1.614	33.784	1.394	34.75	1.355
T4	T323-P	52.97	51.97	1.02	44.38	1.194	37.97	1.395	42.170	1.256	44.07	1.202
T2	T500-P	69.93	67.68	1.03	51.64	1.354	45.06	1.552	52.915	1.321	53.91	1.297
T5	T523-P	79.70	77.18	1.03	62.16	1.282	57.51	1.386	64.730	1.231	65.85	1.210
T7	T524-P	78.99	80.76	0.98	63.88	1.237	60.72	1.301	67.107	1.177	68.85	1.147
T8	T525-P	94.18	89.03	1.06	71.15	1.324	76.61	1.229	78.544	1.199	79.49	1.185
T3	T700-P	91.70	86.89	1.06	57.42	1.597	51.47	1.782	62.357	1.471	60.86	1.507
T6	T723-P	93.41	98.38	0.95	72.40	1.290	72.23	1.293	81.624	1.144	83.12	1.124
Average for TWP				1.014		1.209		1.386		1.255		1.207
R11	R523-U	62.45	68.66	0.91	60.71	1.029	54.66	1.142	57.303	1.090	61.68	1.012
R12	R523-B	71.34	68.84	1.04	60.71	1.175	-	-	-	-	-	-

TWOP is too conservative with an average ratio 1.386, but it seems nominal moments predicted by Eq. (8) suggested by ACI for bonded tendon will be more closer to testing moments with an average ratio 1.209.

(3) Comparing the average ratios 1.209, 1.255 and 1.207 calculated by Eqs. (7)-(9) in Table 3 respectively, those are similar, but it is clear that Eq. (9) proposed by this test would be the easiest and the closest to the testing results.

2. Crack Width

It is well known that the functions of longitudinal mild deformed steel and stirrups in concrete beams are avoiding excessive concentration of cracks and minimizing the cracking width. Similarly, the extent of bonding condition of prestressing tendon will also affect the performance of cracks as mild steel. For comparing reasons, 3 specimens of R5, R9, R10 with TWP are designed with the same amount of longitudinal mild deformed steel and stirrups as specimen R11 with TWOG and specimen R12 with bonded tendon. In the loading process, it is found that R11 beam appears the least number of cracks (7 cracks) and the largest maximum crack width (21.5 cm) during failure, R12 beam appears the most number of cracks (12 cracks) and the smallest maximum crack width (9 cm), and for R5, R9, R10 beams with TWP appear to have 10 to 13 cracks and the maximum crack width 12~13 cm.

The comparison of cracks distribution for these 5 specimens are shown in Fig. 6, and the developments of crack width of 5 specimens at each loading stage are shown in Fig. 7.

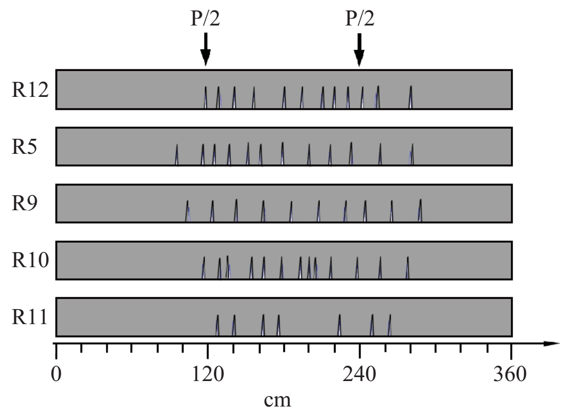

Fig. 6. Comparison of crack distribution.

From the comparisons of Fig. 6 and Fig. 7, both of the distribution and the maximum crack width at each loading stage of R5, R9 and R10 beams with TWP are between R12 (fully bonded) and R11 (TWOG). It reveals that TWP must exists more bonded effects with its surrounding concrete than TWOG, but less bonded effects than bonded tendon. These results also prove that using Eq. (5) to predict f_{ps} would be too conservative for beams with TWP.

By comparing the slope of last segment of each specimen before failure in Fig. 7, the slope of R12 is the steepest that means R12 exists the most bonded forces to restrict the development of cracks than others. Conversely, R11 with TWOG exists no bonded forces to restrict the development

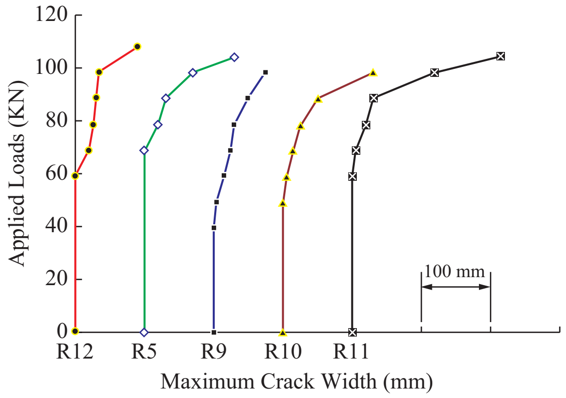

Fig. 7. Comparison of max. crack width *vs*. applied loads.

of cracks, then the slope appears most gradual than others. And the slope of R5, R9, and R10 are between R12 and R11 that shows again the bonded condition of TWP are between TWOG and bonded.

IV. CONCLUSSIONS

The key findings over the course of experimental program are summarized below:

1. Traditionally, both of TWP and TWOG are classified as unbonded tendon and there are no difference for estimating the flexural strength f_{ps} according to ACI 318-08. After a series of structural experiments and analysis, this study proves that the structural behavior of prestressed beams with TWP is between beams with TWOG and beams with bonded tendon. It is too conservative to use Eq. (5) proposed by ACI318-08 to estimating the flexural strength f_{ps} for beams with TWP, and a lower bound modified equation, Eq. (9), is proposed by this study. Using Eq. (9) to estimate the nominal moment Mn for beams with TWP is proved that it has an adequate average safety factor about 1.207.
2. By comparing the number of cracks and maximum crack width before failure for prestressed beams with TWP, TWOG and bonded tendons, it reveals that TWP must exist some bonded effects with its surrounding concrete, and this may be the reason why using Eq. (5) to predict f_{ps} would be too conservative for beams with TWP.
3. Prestressed beams with TWP would be easier to construct and cheaper than beams with TWOG. But from Fig. 7, it shows beams with TWP possess lesser bonded forces than beams with fully bonded tendon. For preventing members from sudden failure, more non-prestressing longitudinal steel and stirrups are recommended.
4. In this study, only beams with a span-to-depth ratio of 35 or less are studied. For slabs with a span-to-depth ratio greater than 35, the difference between slabs with TWP and slabs with TWOG is suggested to be further investigated.

REFERENCES

1. ACI Committee 318 Structural Building Code, *Building Code Requirements for Reinforced Concrete (ACI318M-08) and Commentary*, American Concrete Institute, Detroit, Michigan.
2. Au, F. T. K. and Du, J. S., "Prediction of ultimate stress in unbonded prestressed tendons," *Magazine of Concrete Research*, Vol. 56, No. 1, pp. 1-11 (2004).
3. Baker, A. L. L., "A plastic theory of design for ordinary reinforced and prestressed concrete, including moment redistribution in continuous members," *Magazine of Concrete Research*, Vol. 1, No. 2, pp. 57-66 (1949).
4. Joint ACI-ASCE Committee 423, *Recommendations for Concrete Members Prestressed with Unbonded Tendons*, American Concrete Institute, Farmington Hills, Michigan, p. 25 (2005).
5. Lin, T. Y. and Burns, N. H., *Design of Prestressed Concrete Structures*, 3nd Edition, Wiley, New Jersey, pp. 24-26 (1983).
6. Mattock, A. H., Yamazaki, J., and Kattula, B. T., "Comparative study of prestressed concrete beams with and without tendons," *Proceeding of American Concrete Institute annual convention*, Denver, Colorado, pp. 116-125 (1971).
7. Mojahidin, S. and Gamble, W. L., "Ultimate steel stresses in unbonded prestressed concrete," *American Society of Civil Engineering*, Vol. 104, No. ST7, pp. 1159-1165 (1978).
8. Nilson, A. H., *Design of Prestressed Concrete*, 2nd Edition, Wiley, New Jersey, pp. 14-20 (1987).
9. Warwaruk, J., Sozen, M. A., and Siess, C. P., *Strength and Behavior in Flexure of Prestressed Concrete Beams*, Bulletin No. 464, Engineering Experiment Station, University of Illinois, Urbana, p. 105 (1962).